

## Shape-Control of ZnTe Nanocrystal Growth in Organic Solution

Jun Zhang,<sup>†</sup> Kai Sun,<sup>‡</sup> Amar Kumbhar,<sup>§</sup> and Jiye Fang<sup>\*,†</sup>

Department of Chemistry, State University of New York at Binghamton, Binghamton, New York 13902, Electron Microbeam Analysis Laboratory, University of Michigan, Ann Arbor, Michigan 48109, and Electron Microscope Facility, Clemson University, Anderson, South Carolina 29625

Received: December 15, 2007; In Final Form: February 1, 2008

Precursor-reduction method is employed to synthesize nanometer-sized ZnTe. Zinc blende ZnTe nanocrystals growth in three different shapes under various conditions, that is, quasi-spheres, tetrahedrons, and nanorods, have been observed. It is believed that the crystal growth of ZnTe is the rate-controlling step when superhydride was employed at 250 °C, resulting in quasi-spherical ZnTe nanocrystals. Replacement of superhydride with oleylamine alters the precursor-reduction step as the rate-controlling step, giving tetrahedral ZnTe nanocrystals. At low temperature (150 °C) and in the presence of superhydride and oleylamine, kinetic growth and/or surfactant-template dominate the process, causing an anisotropic crystal growth into ZnTe nanorods. ZnTe nanocrystals are typically surface-active with a similar crystal structure of CdSe. The present study provides a clue to understand the zinc blende-type nanocrystal growth mechanism in high-temperature colloidal system, and may lighten certain strategies of future nanomaterials processing, for example, the synthesis of one-dimensional zinc blende-type semiconductors in solution phase.

### Introduction

It has been reported that characteristics and physical properties of semiconductor and metallic colloids are dependent on their particle size<sup>1</sup> and shape.<sup>2–5</sup> In the past decade, various advanced processing approaches for wet-chemical synthesis and post-treatment techniques have been proposed and developed, demonstrating a success in tuning and control of particle size and size distribution. Compared with the size-control, however, maintenance of particle shape is hard and there still have been plenty of targets to challenge. Most of the traditional strategies for the shape-control of nanocrystals (NCs) are based on the consideration of capping the particle surface with various organic legends/surfactants. Therefore, the crystal growth rate in certain direction could be modified by varying the surface energy on such crystal facet and by elevating the reaction temperature so that the product can be crystallized rapidly and becomes more stable. In this report, we demonstrate our new strategy on the particle shape-control using zinc telluride (ZnTe) colloids as a model system, in which a kinetic approach is involved.

ZnTe is an attractive semiconductor with a direct band gap of 2.1<sup>6</sup>–2.26<sup>7</sup> eV and a Bohr exciton radius of 6.2 nm.<sup>8</sup> Its broad range of potential applications in optoelectronic devices operating in the blue–green region of the spectrum and thermoelectric devices has attracted increasing attention recently.<sup>5,9,10</sup> In addition, the crystal structure of ZnTe is very similar to that of CdSe, a commonly studied semiconductor.<sup>2,11,12</sup> Compared with other semiconductor NCs, however, studies on the preparation of colloidal ZnTe NCs are still limited. Previous studies indicated that a direct reaction between metal zinc (or zinc salts) and tellurium could result in very little ZnTe leaving most reactant unreacted.<sup>10</sup> Li and coworkers<sup>13</sup> concluded that this might be due to the fact that tellurium was not easily reduced

to anions. They employed hydrazine as the reducing agent as well as the solvent and obtained ZnTe Nanorods. In our investigation, we used oleylamine, which acted as a weak reducing agent. Highlighted by this thought, we designed a reaction approach (Scheme 1) in which the Te precursor reduction and NC growth could be “separated” by altering the reducing rate. The feature of this strategy is that the NC shape could be controlled through a variation of the relative growth rates on various crystallographic facets by tuning the concentration of monomers and growth regime when different reducing agents are used.

### Experimental Methods

**General Synthesis.** The syntheses of nanosized ZnTe were typically carried out in a three-neck flask equipped with a condenser under an argon stream.<sup>14</sup> An appropriate amount of zinc precursor (either zinc acetate or zinc chloride) was combined with benzyl ether as solvent in the presence of a certain amount of oleic acid or oleylamine. The system was heated under vigorous agitation. Tellurium-trioctylphosphine (Te–TOP) solution which was pre-prepared by dissolving metallic Te into TOP in a glovebox<sup>15</sup> together with a certain type of reducing agent was subsequently injected into the hot zinc solution. The resultant ZnTe NCs could be isolated after a period of growth time by addition of ethanol followed by centrifugation.

**Chemicals.** Metal tellurium (99.99%), zinc acetate dehydrate (99.999%), trioctylphosphine (TOP, 90%), oleylamine (70%), oleic acid (90%), benzyl ether (99%), dioctyl ether (99%), and super-hydride (LiBH(CH<sub>2</sub>CH<sub>3</sub>)<sub>3</sub>) solution in THF (1 M) are Aldrich products and were used as received. Anhydrous ZnCl<sub>2</sub> was dried in an oven at 130 °C for one week before use. Superhydride solution in dioctyl ether (1 M) was freshly prepared before use according to literature.<sup>16,17</sup>

**Synthesis of ZnTe Quasi-Spheres.** In a typical experiment, zinc acetate dihydrate (1 mmol), benzyl ether (15 mL), and oleic

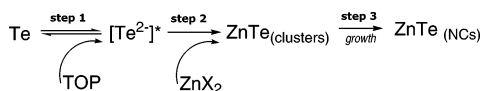
\* Corresponding author. E-mail: jfang@binghamton.edu.

<sup>†</sup> State University of New York at Binghamton.

<sup>‡</sup> University of Michigan.

<sup>§</sup> Clemson University.

### SCHEME 1: Proposed Multisteps in the Synthesis of ZnTe Nanocrystals



acid (1 mL) were mixed and heated to 150 °C for 30 min under vacuum to remove moisture. The temperature was then raised to 250 °C. A mixture of Te–TOP solution (1 mL) and 1 M superhydride solution in dioctal ether (1 mL) was then rapidly injected into this hot solution. The colloidal system was kept at 250 °C for 10 min before being cooled down. Resultant NCs were collected in different periods of time for analyses. The products were separated by adding an excessive amount of ethanol followed by centrifugation. The isolated NCs were re-dispersed in hexane, producing ZnTe colloidal suspensions.

**Synthesis of ZnTe Tetrahedrons.** A 0.408 g sample of ZnCl<sub>2</sub> (3 mmol) was added to the mixture of benzyl ether (15 mL) and oleylamine (3.0 mL) at room temperature, and the resultant solution was heated to 150 °C under vacuum. The homogeneous and clear mixture was then naturally cooled to room temperature. 1 mL of Te–TOP solution (1 M for Te) was subsequently injected into the Zn–oleylamine-containing solution, forming a precursor solution. A 5 mL sample of such precursor solution was injected into 10 mL of phenyl ether which was pre-heated to 250 °C with vigorous stirring, and additional portions of precursor solution (5 mL for each) were similarly injected into the system at intervals of 15 min for a total 3 times. ZnTe tetrahedrons were finally isolated by the addition of an excessive amount of ethanol followed by centrifugation. The NCs were re-dispersed in hexane, forming a clear ZnTe colloidal suspension in yellow.

**Synthesis of ZnTe Nanorods.** A 0.272 g sample of ZnCl<sub>2</sub> (2 mmol) was added to the mixture of benzyl ether (10 mL) and oleylamine (2.0 mL) at room temperature, and the resultant solution was heated to 150 °C under vacuum. The homogeneous and clear mixture was then naturally cooled to room temperature. A 1 M solution of Te–TOP (2 mL) and superhydride solution in dioctal ether (2 mL) were then introduced into this system. Such resultant precursor (5 mL), which was either freshly prepared or aged for 24 h, was added into 10 mL of benzyl ether, gradually heated up to 150 °C, and kept at this temperature for a certain period of growth time, up to 3 h. The separation procedure was the same as that mentioned above.

**Characterization.** Powder XRD was carried out on a PANalytical X'pert diffractometer (CuKα<sub>1</sub> radiation). TEM images were obtained using a JEOL 2010 FEG TEM operating at 200 kV. Optical absorption spectra were recorded on a Cary 50 UV spectrophotometer from Varian Inc.

## Results and Discussion

As described in Experimental Methods, briefly, a zinc salt was dissolved in benzyl in the presence of minor amount of capping and stabilizing agents and was heated to a certain degree of a high temperature. Tellurium-trioctylphosphine (Te–TOP) solution together with a reducing agent (either superhydride or oleylamine) was subsequently injected into this hot zinc solution. We propose that there are at least three equilibriums which exist in this synthesis as illustrated in Scheme 1, that is, a conversion of metallic Te to intermediate state [Te<sup>2-</sup>]<sup>\*</sup>,<sup>15</sup> a fast inorganic formation to ZnTe clusters, and a ZnTe NC growth.

When superhydride as a strong reducing agent was introduced into the Te–TOP system (reaction I) the conversion of Te to [Te<sup>2-</sup>]<sup>\*</sup>, that is, step 1, should complete immediately prior to

the formation (step 2) and growth (step 3) of ZnTe. Furthermore, the [Te<sup>2-</sup>]<sup>\*</sup> should be much more stable because the mass transport is sufficiently rapid. In this case, the rate-controlling step should be the crystal growth (step 3) as the inorganic nucleation (step 2) is usually fast<sup>18</sup> and should not be a rate-determining step. Once the nucleation takes place with a specific crystalline phase, factors from the subsequent growth process (step 3), including the intrinsic surface energy of different crystallographic surfaces, the role of surface selective capping molecules, and others, will affect the final geometry of NCs.<sup>19</sup> Rapid addition of sufficient amount [Te<sup>2-</sup>]<sup>\*</sup> into the Zn system raises the precursor concentration above the nucleation threshold. Although the concentration of the precursors is not high enough to produce any new nuclei as soon as the supersaturation is once relieved by the bursting of a short nucleation,<sup>18</sup> the rest feedstock is sufficient for the consumption of the NC growth. It is generally believed that the NC surface must be a polyhedron containing high-index crystallographic planes which possibly result in a higher surface energy<sup>20</sup> when such a tiny single-phase NC is first nucleated in solution. With further growing in step 3, shape development of the NC is actually dependent on the growth-rate competition on different surface facets dominated by their surface energies. A relatively enriched amount of [Te<sup>2-</sup>]<sup>\*</sup>, kinetically generated by a strong reducing agent (superhydride), can efficiently minimize the growing-rate difference among all of the surface facets, resulting in a tendency of spherical NC formation. Experimentally, when such synthesis was carried out at 250 °C and products were grown for various periods of time, up to 10 min, we observed quasi-spherical ZnTe NCs, indeed. As revealed in Figure 1a, transmission electron microscopy (TEM) images show that the resulting NCs present in shape of quasi-sphere and in average size of ~5 nm when growing for 5 min. The inset in Figure 1a is a selected area electron diffraction pattern of these NCs, indicating a cubic zinc blende crystal structure. High-resolution TEM (HRTEM) image presented in Figure 1d and in Supporting Information Figure S1 reveals the high crystallinity in these NCs. The X-ray diffraction (XRD) pattern of corresponding sample given in Figure 2a verifies the single-phase of zinc blende (or sphalerite) structure [space group (*F*43*m*)(216)] as well. All of the detected peaks are indexed as those from the standard ICDD PDF card (No. 15–0746). Repeat of reaction I in the absence of superhydride resulted in precipitate (bulk ZnTe) at 250 °C or higher temperatures, whereas no product could be harvested at the lower temperature. This supports the proposed mechanism (Scheme 1) on the opposite side, indicating that there might be no intermediate state [Te<sup>2-</sup>]<sup>\*</sup> without superhydride.

To ensure this proposed mechanism, we alternatively replaced the superhydride with oleylamine that is presumably considered as a very weak reducing agent, re-conducted this synthesis by multi-injections<sup>15</sup> of zinc–oleylamine-containing solution into the hot benzyl ether at the same temperature for a total of three times, and extended the growing period of time to 10 min after each injection (reaction II). As expected, tetrahedral ZnTe NCs in an average size of ~15–18 nm were observed (Figure 1b and Supporting Information Figure S2). HRTEM (Figure 1e and Supporting Information Figure S3) clearly shows fcc crystalline structure, and the XRD pattern (Figure 2b) implies that these tetrahedral NCs were well-developed. According to the standard reduction potential, the elemental tellurium has some metallicity and is not easily reduced to the [Te<sup>2-</sup>]<sup>\*</sup> anion.<sup>10</sup> Oleylamine as a weak reducing agent, on the other hand, lacks the capability of completely moving the equilibrium of step 2 to the [Te<sup>2-</sup>]<sup>\*</sup> side. As a result, the rate of “reducing” Te dominates the whole



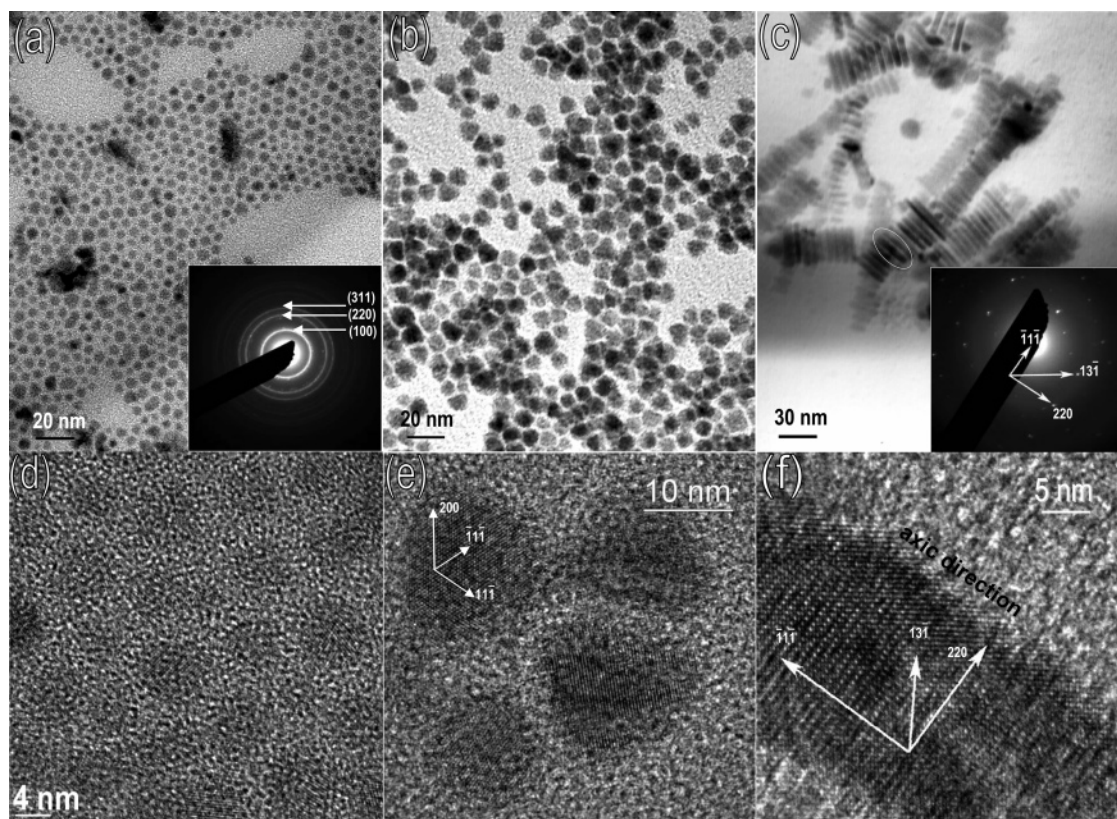


**Figure 1.** Transmission electron microscopy images of ZnTe NCs produced from three reaction pathways: (a) from reaction I, (b) from reaction II, and (c) from reaction III. (d–f) Their high-resolution TEM images, respectively.

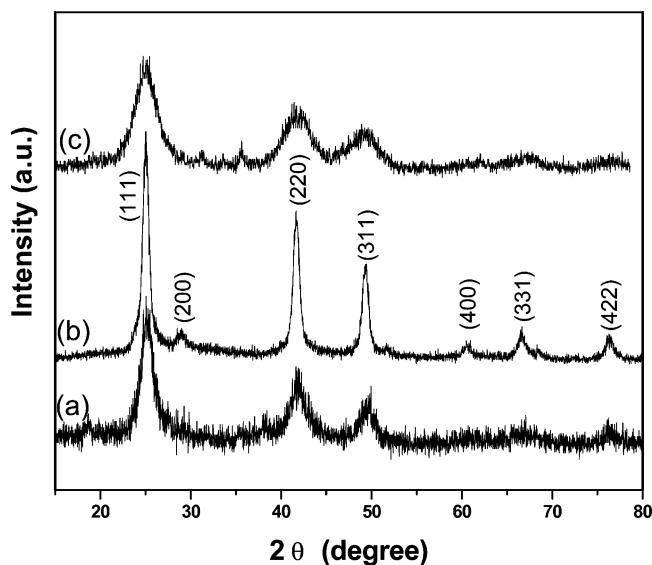


**Figure 2.** XRD patterns obtained from samples produced from three types of reactions: (a) Reaction I, quasi-spherical NCs grown for 2 min; (b) Reaction II, tetrahedral NCs obtained after 3-time injections; (c) Reaction III, 24 h aged ZnTe nanorods. The broaden peaks were caused by the coexisting tiny particle, the minor peaks centered at 31.77, 34.40, and 36.25 degrees could be indexed to those from pattern of ZnO (ICDD PDF Card No. 36–1451).

synthetic process; in other words, step 1 (Scheme 1) becomes the rate-controlling step. The insufficient supplies of  $[\text{Te}^{2-}]^*$  eventually favors the tendency of maximizing the growing-rate difference among different surface facets, say  $\{100\}$  and  $\{111\}$ , at step 3. Actually, a constant multi-injection technique further keeps increasing the portion of the low-index crystallographic planes to reduce the total surface energy and enhances such difference of crystalline development in different facets. It is

believed that the  $\{111\}$  face of a cubic (Kossel) crystal can be classified as a “perfect” K-type face based on thermodynamic consideration,<sup>21</sup> if the chemical potential of the “free” cluster is close to that of the NC (i.e., not too much freshly produced ZnTe clusters are presented). Unlike layer-by-layer growth step on an F-type face, the growth of a K-face is a continuous process based on a consideration of the growth kinetics.<sup>21</sup> In other words, on the surface of the “perfect” K-face, an oncoming cluster immediately finds a kink position to grow and such  $\{111\}$  area enlargement dominates the growth process. Thus, a rapid increase in the area ratio of  $\{111\}$  to other facets eventually results in an evolution of crystal shape to a tetrahedron, which consists of four equivalent  $\{111\}$  planes. To further confirm the role of oleylamine as a weak reducing agent, we have repeated this experiment at 200 °C without oleylamine and other reducing agents, and no NC was produced.

Concerning the step 3, it should be pointed out that the growth regime is an additional critical growth parameter to control the final shape of a NC. At high growth temperature (in our current circumstance, 250 °C), the temperature transportation is characterized by a sufficient supply of thermal energy and the growth generally occurs isotropically from a nucleating core. As a result, zero-dimensional structures (e.g., spheres or tetrahedrons) which are thermodynamically most stable shapes with the lowest overall surface energy are normally anticipated to form, that is the case discussed above. As reported before,<sup>4</sup> the competition of growth regime between thermodynamic and nonequilibrium kinetic growth can be tuned by varying the growth temperature<sup>11,22–25</sup> and by altering the concentration of monomers.<sup>4</sup> In order to focus the investigation on the rate-controlling growth step (step 3) at low temperature, we adopted the synthesis process of spherical ZnTe NCs using superhydride (reaction I), but the experiment was carried out at a temperature as low as 150 °C for 2 h (reaction III). Instead of the ZnTe quasi-spherical

NCs, what we observed were ZnTe nanorods, indicating an anisotropic crystal growth. Figure 1c is a TEM image, showing that the ZnTe NCs are rod-like and well-dispersed, with an average size of  $\sim 5$  nm  $\times$   $\sim 30$  nm. The average diameter of these nanorods is smaller than the Bohr diameter of (bulk) ZnTe (6.2 nm<sup>8</sup>) and much less than those ZnTe nanorods reported previously.<sup>9,10</sup> Inset in Figure 1c is a small angle electron diffraction pattern of these nanorods in a projection direction of  $\langle \bar{1}12 \rangle$ , implying a cubic zinc blende crystal structure. It is worth mentioning that the yield of ZnTe nanorods generated under this low-temperature condition is very limited. To further explore the conditions/mechanism of ZnTe nanorod formation, we have conducted additional experiments in which superhydride was absent while all other reaction parameters/reactants remained the same. As an outcome, the solid product of ZnTe was too little to be collected. In contrast, we have observed that the yield of ZnTe nanorods could also be influenced by the nature of the Te monomers. For example, "aging" of the mixture containing superhydride and tellurium-trioctylphosphine for 24 h before reaction III was carried out could greatly enhance the yield of the resultant ZnTe nanorods with a broadening of rod length and shape distribution (Supporting Information Figure S4). This indicates that sufficient high concentration of monomers is one of the key conditions for the step 3 to produce 1D rods, which is in good agreement with previous reports for the CdSe nanorod system.<sup>2,4,23</sup> It is worth noting that the growth pathways for ZnTe nanorods and for CdSe nanorods are different although tetrahedral NCs of both ZnTe and CdSe<sup>2,4,23</sup> could be obtained under conditions that favor the cubic phase. CdSe nanorods could be a result from a hexagonal growth<sup>2,4,23</sup> with high temperature and high concentration of monomers, whereas growth of ZnTe nanorods could be achieved at relatively low temperature and high concentration of monomers ( $[\text{Te}^{2-}]^*$ ) in our system through the kinetic mechanism proposed above. Unlike the wurtzite structure observed in CdSe rods,<sup>2,4,23</sup> consequently, the ZnTe nanorods show a cubic crystalline phase (Figure 1c,f and Figure 2c). The final shape of NCs could be determined by competitive growth on different types of crystalline facets. On the basis of the analyses of small angle electron diffraction pattern (inset in Figure 1c) and HRTEM image of the "aged" sample (Figure 1f), it can be concluded that the nanorods grow along a  $\langle 111 \rangle$  direction. We therefore suggest that ZnTe nanorods might be a result from the higher growth rate in the  $\langle 111 \rangle$  direction of the preliminary ZnTe nuclei, which is the  $c$  direction of a rod structure. As shown in Supporting Information Figure S4, after an "aging" treatment, the growth of nanorods is always in company with some tiny particles formed from the Te monomers. These extremely small particles which are not easy to separate from the nanorods could be most likely oxidized if being exposed in air for a long time. An XRD pattern of the "aged" nanorods presented in Figure 2c further confirms the presence of such tiny particles. As further evidence, the minor peaks centered at 31.77, 34.40, and 36.25° could be indexed to those from ZnO (ICDD PDF Card No. 36–1451).

Generally speaking, the surface energies on  $\{111\}$ ,  $\{100\}$ , and possibly  $\{110\}$  crystallographic planes in a fcc structure could be distinctive because of the different atomic densities, electronic structures, bindings, and possibly chemical reactivities on them.<sup>20,26</sup> It has also been reported that the  $\{111\}$  crystallographic facets of nanocrystalline rock salts have higher surface energy than  $\{100\}$  planes.<sup>27</sup> The anisotropic growth between the  $\langle 111 \rangle$  direction and others could therefore be possibly attributed to the higher surface energy of the (111) facet over

that of others in zinc blende crystal structure of fcc ZnTe. To further differentiate whether or not the kinetic growth is the major reason resulting in the formation of nanorods, we have alternately repeated reaction I under the same conditions but with a longer period of growth times up to 3 h. No nanorod was ever identified. For example, a TEM image shows that growth for 1 h results in agglomeration of spherical NCs, rather than elongated rods (Supporting Information Figure S5), revealing that the growth mechanisms at 250 °C and at 150 °C are different. Additional contribution to the formation of ZnTe nanorods in the direction of  $\langle 111 \rangle$  as  $c$  axis could probably be the template of surfactant(s). At relatively low temperature, different binding abilities of surfactant(s) on (111) and on other facets could be a partial (or full) driving force<sup>3,24</sup> causing the fast growth in the direction  $\langle 111 \rangle$ , that is,  $c$  axis of a rod. Such selective capping interaction sometimes even can alter the sequence of surface energies associated with various crystallographic planes.<sup>28</sup> For instance, Jun et al. reported that injecting a single-source precursor of ZnTe into a mixed-surfactant solution produced rod-like ZnTe NCs.<sup>29</sup> They proposed that the surfactants formed rod-like micelles that could template the one-dimensional crystal for growth. Manna et al. also demonstrated that anisotropic growth of several semiconductors could be achieved by presenting two surfactants with significantly different binding abilities to NC faces, leaving only one facet with preferential growth rate.<sup>12,23</sup> For example, phosphonic acid is known to slow the growth of CdSe NCs and to induce preferential growth along the  $c$  axis of the wurtzite structure, producing CdSe nanorods.<sup>2</sup> Although it is hard to quantitatively distinguish the major capping contribution among oleic acid, oleylamine, and TOP in our system, it seems that TOP acts as a dominant capping agent in binding on the surface of ZnTe NCs on the basis of the following two facts that we observed. First, without addition of oleylamine, discrete quasi-spherical ZnTe NCs could still be obtained in the presence of TOP and oleic acid (reaction I, Figure 1a); second, we realize that the yellow colloidal suspensions of both quasi-spherical NCs produced from reaction I and tetrahedral NCs obtained from reaction II could gradually turn dark brown after 1 to 2 days because of the particle aggregation.<sup>30</sup> If 1 or 2 drops of TOP were added into the colloidal system (about 10 mL suspensions) immediately after the synthesis, the aggregation process could be ceased, whereas addition of either oleic acid or oleylamine did not stop the aggregation.

Figure 3 exposes UV–vis absorption spectra of various ZnTe NCs. Curves a–d were recorded from those quasi-spherical ZnTe NCs synthesized from reaction I (250 °C) and grown for 45 s, 2 min, 5 min, and 10 min, respectively. As displayed, a distinguishable absorption peak ranged around 430 nm can be determined when the NCs were grown for 45 s. The appearance of absorption peak is a sign that the as-prepared NCs are moderately monodisperse. This peak progressively shifts to a longer wavelength and gradually alters to shoulder-like curves<sup>29</sup> as the growth time increases, indicating that relatively broader size distributions could be a result as the growth time is prolonged. The red-shift of absorption with the increasing growth time is associated with an increase of particle size because of the continuous growth of NCs. As shown in e and f, absorption shoulders are further shifted toward the direction of long wavelength when larger ZnTe nanorods (reaction III,  $\sim 5$  nm  $\times$   $\sim 30$  nm) and tetrahedrons (reaction II, 15–18 nm in size) were examined.



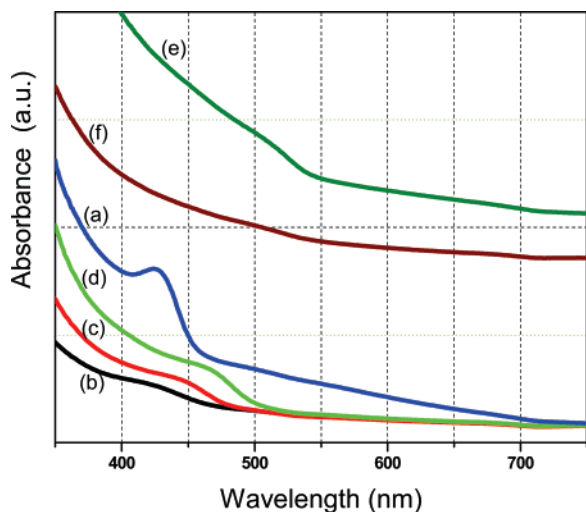
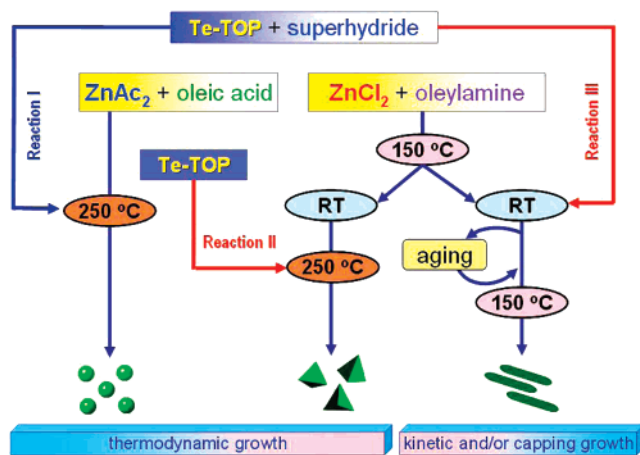


**Figure 3.** Optical absorption spectra collected on various ZnTe samples. (a–d) Quasi-spherical ZnTe NCs synthesized from Reaction I and grown for 45 s, 2 min, 5 min, and 10 min, respectively; (e) 15–18 nm tetrahedral ZnTe NCs produced from Reaction II; (f) 24 h aged ZnTe nanorods prepared from Reaction III.

### SCHEME 2: Flow Chart of Shape-Controlled Synthesis of ZnTe Nanocrystals



### Conclusions

In conclusion, three types of ZnTe NC growth have been discussed and outlined in Scheme 2. It is realized in our system that the crystal growth is the rate-controlling step when superhydride was employed at 250 °C, resulting in quasi-spherical ZnTe NCs. Replacement of superhydride with oleylamine might alter the precursor-reduction as the rate-controlling step, favoring the tendency of maximizing the growth-rate difference among different surface facets and giving tetrahedral ZnTe NCs. At low temperature (150 °C) and in the presence of superhydride and oleylamine, kinetic growth and/or surfactant template may dominate the process, resulting in ZnTe nanorods through an anisotropic crystal growth. In any case, only cubic ZnTe NCs were obtained. In addition, TOP is identified as a kind of major capping ligands among other organic components.

**Acknowledgment.** This work was supported by NSF CAREER program (DMR-0449580/0731382), DOE SBIR project (DE-FG02-07ER86296) and State University of New York at Binghamton. We thank Dr. Jibao He for his help in structural analysis.

**Supporting Information Available:** High-resolution TEM image of ZnTe quasi-spherical nanocrystals synthesized from pathway of Reaction I (Figure S1), TEM image of ZnTe tetrahedral nanocrystals synthesized from pathway of Reaction II (Figure S2), high-resolution TEM image of ZnTe tetrahedral nanocrystals synthesized from pathway of Reaction II, (Figure S3), TEM image of ZnTe nanorods synthesized from pathway of Reaction III. The precursors as described in the context were aged for 24 h (Figure S4), and TEM image showing agglomeration of quasi-spherical ZnTe nanocrystals synthesized from pathway of Reaction I. The growth time is 1 h (Figure S5). This material is available free of charge via the Internet at <http://pubs.acs.org>.

### References and Notes

- (1) Murray, C. B.; Sun, S.; Gaschler, W.; Doyle, H.; Betley, T. A.; Kagan, C. R. *IBM J. Res. Dev.* **2001**, *45*, 47–56.
- (2) Peng, X.; Manna, L.; Yang, W.; Wickham, J.; Scher, E.; Kadavanch, A.; Alivisatos, A. P. *Nature* **2000**, *404*, 59–61.
- (3) Jun, Y.-w.; Seo, J.-w.; Oh, S. J.; Cheon, J. *Coordin. Chem. Rev.* **2005**, *249*, 1766–1775.
- (4) Manna, L.; Scher, E. C.; Alivisatos, A. P. *J. Clust. Sci.* **2002**, *13*, 521–532.
- (5) Lee, S. H.; Kim, Y. J.; Park, J. *Chem. Mater.* **2007**, *19*, 4670–4675.
- (6) Huang, X.; Li, J.; Fu, H. *J. Am. Chem. Soc.* **2000**, *122*, 8789–8790.
- (7) Mahalingam, T.; John, V. S.; Rajendran, S.; Sebastian, P. J. *Semicond. Sci. Technol.* **2002**, *17*, 465–470.
- (8) Li, L.; Yang, Y.; Huang, X.; Li, G.; Zhang, L. *J. Phys. Chem. B* **2005**, *109*, 12394–12398.
- (9) Yong, K.-T.; Sahoo, Y.; Zeng, H.; Swihart, M. T.; Minter, J. R.; Prasad, P. N. *Chem. Mater.* **2007**, *19*, 4108–4110.
- (10) Du, J.; Xu, L.; Zou, G.; Chai, L.; Qian, Y. *J. Cryst. Growth* **2006**, *291*, 183–186.
- (11) Peng, Z. A.; Peng, X. *J. Am. Chem. Soc.* **2001**, *123*, 1389–1395.
- (12) Shieh, F.; Saunders, A. E.; Korgel, B. A. *J. Phys. Chem. B* **2005**, *109*, 8538–8542.
- (13) Li, Y.; Ding, Y.; Wang, Z. *Adv. Mater.* **1999**, *11*, 847–850.
- (14) Liu, Q.; Lu, W.; Ma, A.; Tang, J.; Lin, J.; Fang, J. *J. Am. Chem. Soc.* **2005**, *127*, 5276–5277.
- (15) Lu, W.; Ding, Y.; Chen, Y.; Wang, Z. L.; Fang, J. *J. Am. Chem. Soc.* **2005**, *127*, 10112–10116.
- (16) Fang, J.; Stokes, K. L.; Zhou, W. L.; Wang, W.; Lin, J. *Chem. Commun.* **2001**, 1872–1873.
- (17) Sun, S.; Murray, C. B. *J. Appl. Phys.* **1999**, *85*, 4325–4330.
- (18) Murray, C. B.; Kagan, C. R.; Bawendi, M. G. *Annu. Rev. Mater. Sci.* **2000**, *30*, 545–610.
- (19) Jun, Y.-w.; Lee, J.-H.; Choi, J.-s.; Cheon, J. *J. Phys. Chem. B* **2005**, *109*, 14795–14806.
- (20) Wang, Z. L. *J. Phys. Chem. B* **2000**, *104*, 1153–1175.
- (21) Mutafschiev, B. *The atomistic nature of crystal growth*; Springer: Berlin, 2001; Vol. 43.
- (22) Lu, W.; Fang, J.; Stokes, K. L.; Lin, J. *J. Am. Chem. Soc.* **2004**, *126*, 11798–11799.
- (23) Manna, L.; Scher, E. C.; Alivisatos, A. P. *J. Am. Chem. Soc.* **2000**, *122*, 12700–12706.
- (24) Lee, S.-M.; Jun, Y.-w.; Cho, S.-N.; Cheon, J. *J. Am. Chem. Soc.* **2002**, *124*, 11244–11245.
- (25) Jun, Y.-w.; Jung, Y.-y.; Cheon, J. *J. Am. Chem. Soc.* **2002**, *124*, 615–619.
- (26) Xiong, Y.; Xia, Y. *Adv. Mater.* **2007**, *19*, 3385–3391.
- (27) Lee, S.-M.; Cho, S.-N.; Cheon, J. *Adv. Mater.* **2003**, *15*, 441–444.
- (28) Xia, Y.; Yang, P.; Sun, Y.; Wu, Y.; Mayers, B.; Dates, B.; Yin, Y.; Kim, F.; Yan, H. *Adv. Mater.* **2003**, *15*, 353–389.
- (29) Jun, Y.-w.; Choi, C.-S.; Cheon, J. *Chem. Commun.* **2001**, 101–102.
- (30) Note: all of the particles were “washed” for several times after the synthesis using a pair of solvents consisting of hexane and ethanol in order to get rid of reaction solvent and bi-products. As a result, the capped organic ligands should be partially removed as well.